Aerosol and Air Quality Research, 13: 608–617, 2013

ISSN: 1680-8584 print / 2071-1409 online
doi: 10.4209/aaqr.2012.07.0183

A Sampling Train for Rapid Measurement of Regional Lung Deposition

Kuang-Nan Chang[1], Sheng-Hsiu Huang[1], Chun-Wan Chen[2], Huey-Dong Wu[3], Yu-Kang Chen[4], Chane-Yu Lai[5], Chih-Chieh Chen[1*]

[1] *National Taiwan University, Taipei, Taiwan*
[2] *Institute of Occupational Safety and Health, New Taipei City, Taiwan*
[3] *National Taiwan University Hospital, Taipei, Taiwan*
[4] *Chang Jung Christian University, Tainan, Taiwan*
[5] *Chung Shan Medical University, Taichung, Taiwan*

ABSTRACT

An experimental system for rapid measurement of regional lung deposition of Di-2-ethylhexyl sebacate (DEHS) aerosol particles was established in the present study. The principal goal was to identify the most relevant components of the sampling train and the proper instruments to be employed. After completing the search for an optimal sampling train and instruments, a human subject test was performed. Overall, the sampling train consisted of a mouthpiece, flow meter, and particle counter. The mouthpiece was attached to a Fleisch pneumotachograph. Several TSI condensation particle counters (CPCs), a PC-LabCard and a personal computer were employed to measure and record the counts of test particles at 100 Hz. A cylinder-piston breathing machine was built to generate a series of "standard" breathing patterns. For non-human subject tests, an acrylic tube, 5 cm diameter × 60 cm length, packed with a piece of 100 ppi foam disks was used as a substitute for the human respiratory tract. The optimal sampling train was determined to be a 1TH Fleisch pneumotachograph with a CPC model 3025A because of its short response time and low flow fluctuation. A healthy non-smoking man volunteered to be the subject, and was asked to follow breathing patterns generated by a cylinder-piston breathing machine. The local deposition efficiency was calculated for 1 μm DEHS particles of each 50 cm^3 volumetric region. The deposition data showed a good agreement with previous studies. Compared to the conventional bolus system, the advantage of the rapid measurement system developed in this work is its simplicity, low exposure, and high efficiency.

Keywords: Lung deposition; Pneumotachograph; Aerosol sampling.

INTRODUCTION

Inhalation is the most important route of entry for atmospheric aerosol. Further, it is necessary to determine the specific region of particle deposition in the respiratory tract for properly evaluating human health risk. For example, a larger particle such as pollen may deposit in the upper airway and merely cause a sneeze, while smaller particles could deposit in the alveoli and result in serious diseases. The physical factors that result in differences in regional lung deposition are similar to those of particles collecting on a filter. However, filtration normally occurs under a steady flow rate, while the living body is a complex system of changing geometry, unsteady flow rates, and variable flow directions resulting from the breathing cycle.

Several methods have been developed to determine lung deposition in humans. Total deposition measurements estimated the intake dose by comparing the aerosol concentrations in inhaled and exhaled air (Heyder *et al.*, 1973; Heyder *et al.*, 1975; Yu and Diu, 1983; Tu and Knutson, 1984; Brand *et al.*, 2000; Jaques and Kim, 2000; Kim and Jaques, 2004; Montoya *et al.*, 2004; Kim and Jaques, 2005; Löndahl *et al.*, 2006). These data are useful to determining the overall dose of therapeutic or toxic aerosols a person has received. However, local deposition measurements provide detailed information on the longitudinal regional distribution of deposition within the respiratory tract.

To gain a more detailed assessment of regional lung deposition, researchers have employed methods such as the artificial model (cast) of the human respiratory tract (Chan and Lippmann, 1980; Grgic *et al.*, 2006; Su and Cheng, 2006; Ali *et al.*, 2008; Zhou *et al.*, 2011), inhalation of particles labeled with γ-emitting radionuclide (Lippmann and Albert, 1969; Stahlhofen *et al.*, 1980; Hashish *et al.*, 1998; Möller *et al.*, 2006), and mathematical models (Yu and Diu, 1983; ICPR, 1994; Asgharian *et al.*, 2006; Park and Wexler,

* Corresponding author. Tel.: +886-2-33668086;
Fax: +886-2-23938631
E-mail address: ccchen@ntu.edu.tw

2007, 2008; Luo and Liu, 2009). Such studies have confirmed aerosol deposition in the respiratory tract is strongly influenced by aerosol size, aerosol charge distribution, and breathing pattern (Heyder *et al.*, 1980; Blanchard and Willeke, 1983; Yu and Diu, 1983; Kim and Jaques, 2004; Kim and Hu, 2006; Ali *et al.*, 2008; Park and Wexler, 2008) and lung morphometric parameters (Cheng *et al.*, 1996; Hofmann *et al.*, 1999). However, all these methods have limitations. A hollow cast is not equivalent to a living organ. Methods involving inhalation of aerosol particles labeled with γ-emitting radionuclide are cumbersome and expose human subjects to radioactive substances. Mathematical and computer models are developed on the basis of simplified airway geometry and flow conditions to shorten computation time, and therefore, need to be validated by experimental data.

The serial bolus delivery technique, developed about three decades ago, is a non-invasive physiological lung test, involving injection of small volumes of monodisperse aerosols (the bolus) into predetermined volumetric in vivo lung regions of humans during inhalation of clean, aerosol-free air (Kim *et al.*, 1996; rand *et al.*, 1997; Heyder *et al.*, 1988; Grgic et al., 2006). The difference in the spread of the bolus between inspiration and expiration is evaluated via plots of aerosol concentration versus respired volume and is thought to be closely related to the conditions of the convective flow in the lungs. In addition to determining regional deposition of inhaled particles, the aerosol bolus technique is also a promising tool for detecting early lung impairment in individuals (McCawley and Lippmann, 1988; Rosenthal et al., 1992; Westenberger *et al.*, 1992; Anderson *et al.*, 1994; Brand *et al.*, 1994). However, the aerosol bolus dispersion process is time-consuming because only one aerosol size and one regional deposition efficiency can be measured at a time. Another disadvantage is a high concentration of challenge aerosols is needed to ensure the accuracy and precision of the measurement. For the bolus method, the normal aerosol concentrations range from 2×10^3 to 4×10^4 particles/cm^3, depending on the size of the challenge aerosols (Kim *et al.*, 1996).

Single-breath inhalation experimentation has been advocated as an alternative for measuring longitudinal distribution of deposited particles in the respiratory tract, and for investigating the influence of lung diseases (Brand *et al.*, 1999). This single-breath technique is now even more convincing with advances in aerosol instrumentation, allowing higher sampling rates and better aerosol size resolution. However, there is still no accepted standardized method. The aim of the present study was to develop and optimize a sampling train to work with commercially available aerosol instruments for rapid measurement of regional lung deposition, which, hopefully, will lead to a standard methodology.

EXPERIMENTAL MATERIALS AND METHODS

To follow the concept of a single breath, the optimal design of the experimental apparatus was to shorten the response time of the sampling train. The optimization process also considered the sampling rate and flow fluctuation of the aerosol instruments employed in this work. After the test system was optimized, human tests were conducted to validate the design. Each test was repeated at least 5 times.

Optimization of the Sampling Train

The test apparatus was divided into three parts: aerosol generation, aerosol measurement and sampling train, as shown in Fig. 1. To produce a steady concentration of monodisperse aerosol, a condensation monodisperse aerosol generator (Model 3075, TSI Inc., St. Paul, MN, U.S.A.) was used. Di-2-ethylhexyl sebacate (DEHS)-ethanol solution was used as the test agent. Before being introduced into the mixing chamber, the aerosol output was neutralized by passing through an annular 25 mCi Am-241 radioactive source. The cylindrical mixing chamber consisted of an aluminum tube with a height of 180 cm and diameter of 7.8 cm. An aerosol free dilution air was injected into the mixing chamber at test flows ranging from 15 to 100 L/min, equivalent to duct velocity from 0.05 to 0.35 m/s (flow rate/cross sectional area of the duct). The relative humidity (RH) of the dilution air was conditioned to carry relative humidity of 70 to 80%, for the comfort of the subjects. All air flows were controlled using mass flow controllers (Teledyne Hastings Instruments, Hampton, VA, U.S.A.) and calibrated with an electronic bubble meter (Gilibrator, Gilian Instrument Crop., Wayne, NJ, U.S.A.) or a homemade spirometer (for flow higher than 30 L/min). A scanning mobility particle sizer (SMPS; Model 3936, TSI Inc.) and an aerodynamic particle sizer (APS, Model 3321, TSI Inc.) were used to monitor the aerosol number concentration and size distribution. The particle concentration was about 3000 #/cm^3 in the mixing chamber when the dilution flow was 100 L/min.

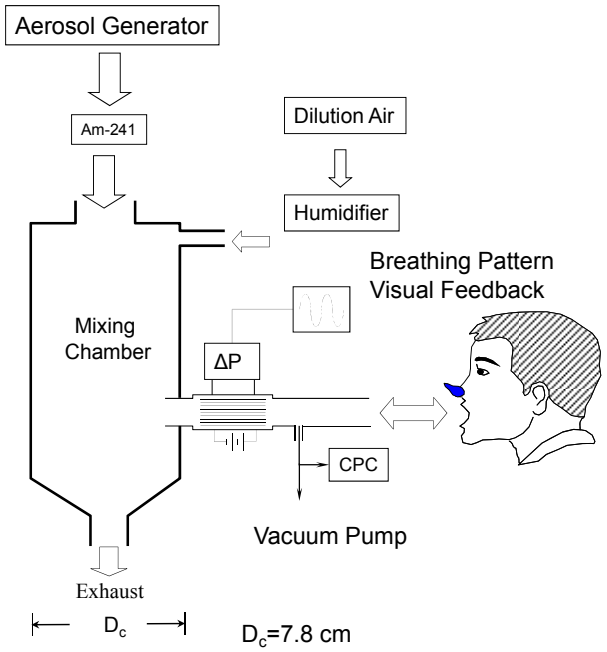

Fig. 1. Schematic diagram of the experimental system set-up.

The main sampling train consisted of a mouthpiece, a flow meter, and a particle counter. The mouthpiece was attached to the flow meter to have a minimum dead space. In the present study, TSI condensation particle counters (CPCs) were used to measure the particle number concentrations. During respiration, aerosol particles were sampled continuously from the sampling train into a CPC via T-port attached to the mouthpiece. By using a PC-LabCard (PCI-1710HG-A, Advantec Inc., Taipei, Taiwan) and a personal computer, the CPC could measure the particle number count at a frequency of 100 Hz. To optimize the experimental system, combinations of three different models of TSI CPCs (Model 3010, 3022A, and 3025A) with three Fleisch pneumotachograph flow meters: Fleisch 1TH (P_1), 0TH (P_0), and 00TH (P_{00}), and two home-made flow meters (P_{h1} and P_{h2}) were compared for response time and flow rate fluctuation of CPCs at different pressure drop conditions. The detailed dimensions of these sampling probes are listed in Table 1. In order to avoid condensation on the sampling train, the flow meter was heated to slightly higher than 37°C. Low sampling frequencies were arbitrarily chosen for in this part of experiment. The 5.4 bpm (breath per minute) was randomly picked to enhance and demonstrate the dead space effect due to sampling probes and pneumotachograph flow meters.

The CPC flow rate fluctuations and pressure drop curves were recorded using pressure transducers (PX653-2.5BD5V, Omega Engineering Inc., Stamford, CT), which were connected to a PC-LabCard and a personal computer. The pressure transducers were calibrated against an inclined manometer. A cylinder-piston type of breathing machine was used to generate a series of sinusoidal breathing patterns of different breathing frequencies and tidal volumes. Cyclic flows are easier than constant flows for subjects to follow because it is difficult to accelerate from zero to a constant flow in a short period of time. An acrylic tube, 5 cm diameter × 60 cm length, packed with 100 ppi (pore per inch) foam disks was used as a substitute for the human respiratory tract, to simulate lung deposition during this part of the experiment. The collection efficiency of foam disk was not exactly the same as the particle deposition efficiency in human respiratory tract, but the trend of the particle deposition was similar. The main purpose of this simulated lung was to test the response time of the sampling train and the aerosol measurement instruments, not to compare with the human lung deposition.

Table 1. The list of CPC models and sampling probes.

CPC models and flow modes		
CPC model	High Flow	Low Flow
3010	X	1
3022A	1.5	0.3
3025A	1.5	0.3

Flow rate: L/min

Sampling probes and volume			
Probe	Diameter	Length	Volume
In-house 1 (P_{h1})	0.26	12.8	2.82
In-house 2 (P_{h2})	0.50	10.5	8.25
00TH (P_{00})	0.48	15.0	8.94
0TH (P_0)	0.50	15.0	11.78
1TH (P_1)	0.85	14.5	45.46

Unit: cm, Volume: cm^3

Human Subject Test

The regional lung deposition measurements were made with the sampling train, which was optimized according to the procedures described in part a. A healthy non-smoking man (age 30 yr, height 160 cm, weight 63 kg) volunteered to be the subject. The breathing patterns generated by the cylinder-piston breathing machine were shown on a monitor in front of the subject for him to follow. It took about an hour for the subject to practice and to follow the breathing curves reasonably well, within 5% error per breathing cycle. The aerosol deposition data of the deviated breathing cycle were removed manually during data analysis.

To calculate the longitudinal distribution of aerosol deposition, tidal volume can be divided into infinitesimally small volume elements, or n elements. Aerosol particles within each volume element of the respiratory tract system are assumed to deposit with an efficiency of x_i as they are inhaled and exhaled again with the same deposition efficiency penetrating through the same volume element (i) (Kim *et al.*, 1996; Brand *et al.*, 1999). Aerosol recovery from the i_{th} volume element, RC*i*, can be obtained by

$$RC_i = \prod_{k=1}^{i} (1 - x_k)^2 \quad (1)$$

Notice that aerosol deposition fraction in i_{th} volume element (DF_i) is the sum of depositions during inspiration and expiration. The local deposition fraction in the i_{th} volume element, LDF_i, can be expressed as

$$LDF_i = \frac{1}{n} \sum_{j=1}^{n} DF_i \quad (2)$$

RESULTS AND DISCUSSION

The airflow rate in the mixing chamber needed to be high enough, to prevent the exhaled breath, normally with lower aerosol concentration due to lung deposition, from being re-sampled, because it might interfere with the calculation of regional lung deposition based on the recovery model. Fig. 2 shows four curves of normalized aerosol concentrations (particle concentration sampled/particle concentration in the mixing chamber) of four different dilution air flow rates, during a breathing cycle with a tidal volume of 500 mL and an arbitrary breathing frequency of 10.5 breath/min (bpm). At the beginning of the inhalation phase, particle concentration apparently increased with increasing duct velocity. This occurred because higher chamber aerosol flow flushed the clean exhaled air more completely. Therefore, the 'response time' to reach the chamber aerosol concentration decreased with increasing chamber airflows. The effect of airflow was especially significant when the flow was lower than 50 L/min

(0.18 m/s), but not as significant for a flow rate higher than 50 L/min. However, to achieve the faster response time, the dilution flow rate was set at 100 L/min in the present study.

Three models of CPCs (TSI 3010, 3022 and 3025) operated under either high or low flow mode, were tested for response time. To obtain the near-real response time, filtered airflow slightly higher than the sampling flow of particle counter was introduced into the sampling train to assure the particle counter did not sample any particles, as shown in Fig. 3. Once the filtered airflow was turned off, the aerosol concentration increased with time and eventually reached the same level as in the mixing chamber. Depending on the volume and sampling flow rate of the sampling train of each particle counter, the CPCs in order of response from fastest to slowest were 3025-H (High flow), 3010, 3022-H, 3025-L (Low flow), and 3022-L. The response (from 0 to 95%) of CPC 3025-H was about 1 second, 3.5 times faster than 3010 and 3022-H. Consequently, the CPC 3025-H was selected for subsequent experiments.

The pneumotachograph posed the most significant part of air resistance of the whole sampling train. A large flow meter normally caused a lower pressure drop, but the large volume resulted in a longer response time. Therefore, two smaller homemade flow meters, together with three Fleisch pneumotachographs (shown in Table 1) were tested to decide the best one to be installed in the system. The pressure drop curves of five flow meters at a tidal volume of 500 mL and 9 bpm were shown in Fig. 4. The three Fleisch pneumotachographs delivered a more symmetrical curve than the homemade flow meters during a full cycle of

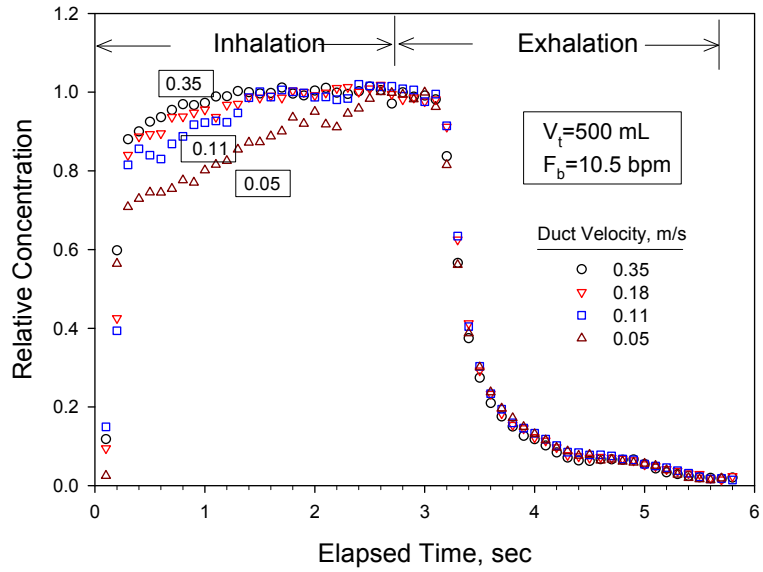

Fig. 2. Effect of dilution air flow on the response time to reach stable aerosol concentration.

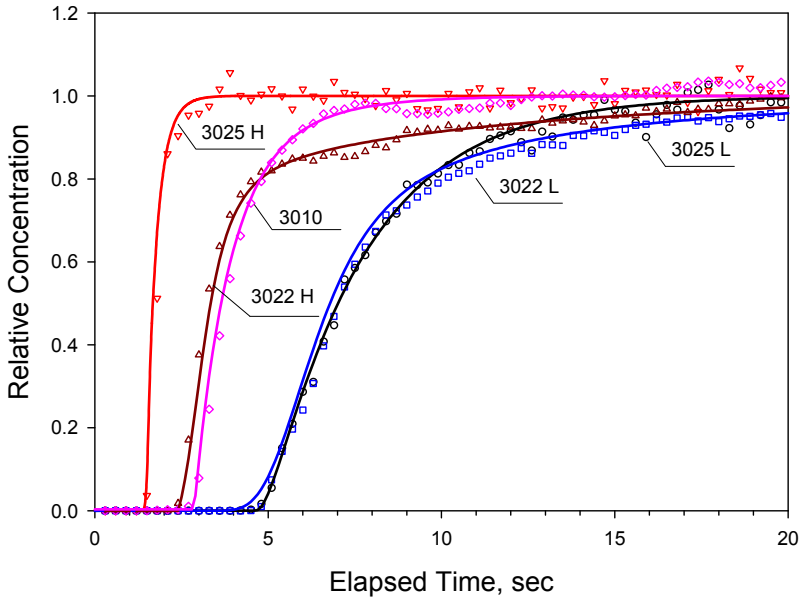

Fig. 3. Particle concentration response times of different CPC models and flow modes.

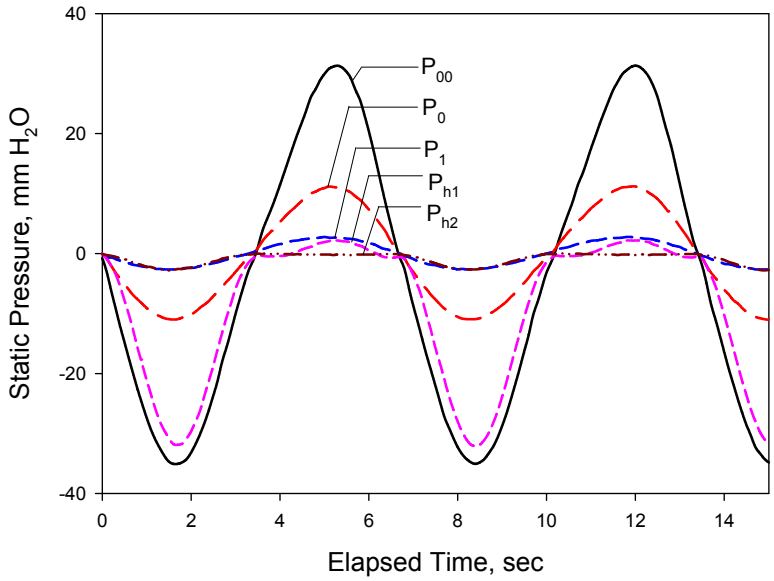

Fig. 4. The static pressure curves of different sampling probes.

breathing. This was because the homemade flow meters only measured a single static pressure, while the Fleisch pneumotachograph flow meters measured the difference between two static pressures. The asymmetrical pressure curves were difficult for human subjects to follow, especially for the low signal period. On the other hand, the P_{00} Fleisch pneumotachograph, the smallest flow meter, posed the highest pressure drop, and became a serious challenge to the internal pump of CPC, especially during a breathing cycle. The flow fluctuation acting on the CPC might affect particle concentration measurement. A flow rate higher than the manufacturer's recommendation might produce higher particle concentrations, and vice versa, with lower flow rates resulting in lower concentrations. According to the TSI CPC design, a flow rate would be considered inappropriate (error message, lamp on) if it was over ± 10% of the recommended value. This criterion was employed to judge whether the CPC flow rate fluctuation was acceptable. However, it was not easy to monitor the CPC flow rate directly in real time. Therefore, the CPC sampling inlet pressure was monitored instead, to record the fluctuation in the CPC flow rate.

In theory, the largest diameter tube, i.e., P_1 Fleisch pneumotachograph would alleviate the flow fluctuation in the CPC during the breathing cycle. However, the large tube also caused a longer response time because of larger volume, as shown in Fig. 5. Similar to the system used in Fig. 3, the CPC sampled filtered air (5 L/min) to record a zero particle count. The excess flow was pushed into the chamber. Once the 3-way valve turned off, the CPC started sampling aerosols from mixing chamber. The sampling train had a maximum volume of 45 cm^3 (dead space) when equipped with P_1 Fleisch pneumotachograph and caused an approximately 1 second lag in response time for CPC model 3025 (high flow mode). The response times of pneumotachographs P_0 and P_{00} were much shorter due to smaller dead space.

However, the effect of dead space on the response time of CPC measurement was not significant when the sampling train was attached to the breathing machine, when operated under a tidal volume of 500 mL and breathing frequency of 5.4 bpm. The particle concentration response times of three probes were almost the same, as shown in Fig. 6. This was because the flow rate generated by the breathing machine dominated and weakened the difference among the different sized flow meters.

For the cases of higher breathing flow (i.e., higher tidal volume and breathing frequency) the particle concentration fluctuated more significantly during the inhalation when the sampling train was incorporated with a P_{00} Fleisch pneumotachograph, as shown in Fig. 7. The fluctuation in particle number concentration increased with increasing breathing frequency (from 10 to 15 bpm) and tidal volume (from 500 to 800 mL) during inhalation. This was apparently due to the fluctuation in the CPC flow rate. Therefore, the P_1 Fleisch pneumotachograph was recommended to reduce the effect of pressure drop change on the CPC sampling flow, especially when the breathing flow was high.

The working ranges of the three Pneumotachographs in terms of breathing patterns are shown in Fig. 8. The CPC inlet pressure drop was under the maximal pressure drop during breathing cycles. The error (Lamp on) of CPC 3025 flow fluctuation was less than ± 10% if the CPC inlet pressure drop was lower than –13 mm H_2O for the P_1 Fleisch pneumotachograph. For example, the maximum acceptable breathing frequency for P_1 Fleisch pneumotachograph was about 15 bpm with a tidal volume of 800 mL. Pneumotachographs P_0 and P_{00} can only be used under unusually low breathing frequencies, less than 11 and 6 bpm, respectively. Based on the data shown in Figs. 5–8, the largest flow meter P_1 is strongly recommended when considering both response time and flow fluctuation.

To validate the effectiveness of this sampling train, monodisperse 1-μm DEHS particles were used as the test

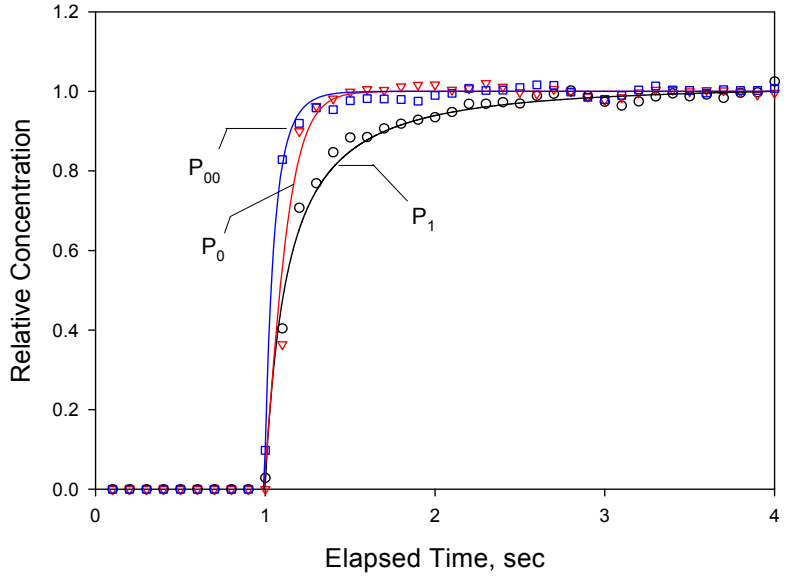

Fig. 5. Particle concentration response times of different sampling probes.

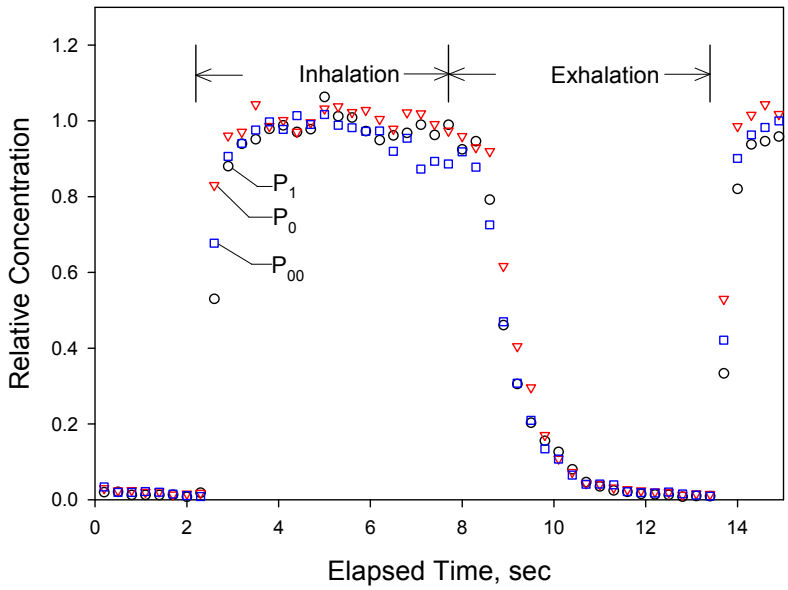

Fig. 6. Effect of dead space on the response time of different sampling probes. This experiment was performed using a breathing machine and a piece of foam simulating human lung.

agent in a regional lung deposition measurement for a young male volunteer. He was asked to follow a breathing pattern (tidal volume 500 mL, breathing frequency 15 bpm) generated using a breathing machine. The particle concentration in the mixing chamber was about 1000–3000 #/cm^3. Fig. 9 shows the local deposition values for each 50 cm^3 volumetric regional as a function of penetration volume. These data were repeated more than five times. The local deposition efficiency was calculated for each 50 cm^3 volumetric region to compare with the data reported by Kim *et al.* (1996). Our data agreed well with Kim's data (solid line), except in the deep lung (400–500 mL), i.e., alveolar region. The higher deposition efficiency in the deep lung was very repeatable using the experimental apparatus developed in this work. This high deposition efficiency is likely due to the 'dilution effect' of functional residual capacity (FRC), where the aerosol concentration was expected to be low due to the long retention time in that region. For some reasons, this dilution effect was not shown in Kim's experiment using the bolus technique probably because Kim's study employed a single-breath method that involved maximal expiration to RV (Residual volume). Therefore, the local deposition efficiency value in deep region (400–500 mL) measured in this this work was higher than Kim's.

In theory, inertial impaction plays an important role in the first few generations of bifurcation where the velocity is high. For the rest of the respiratory airways, the

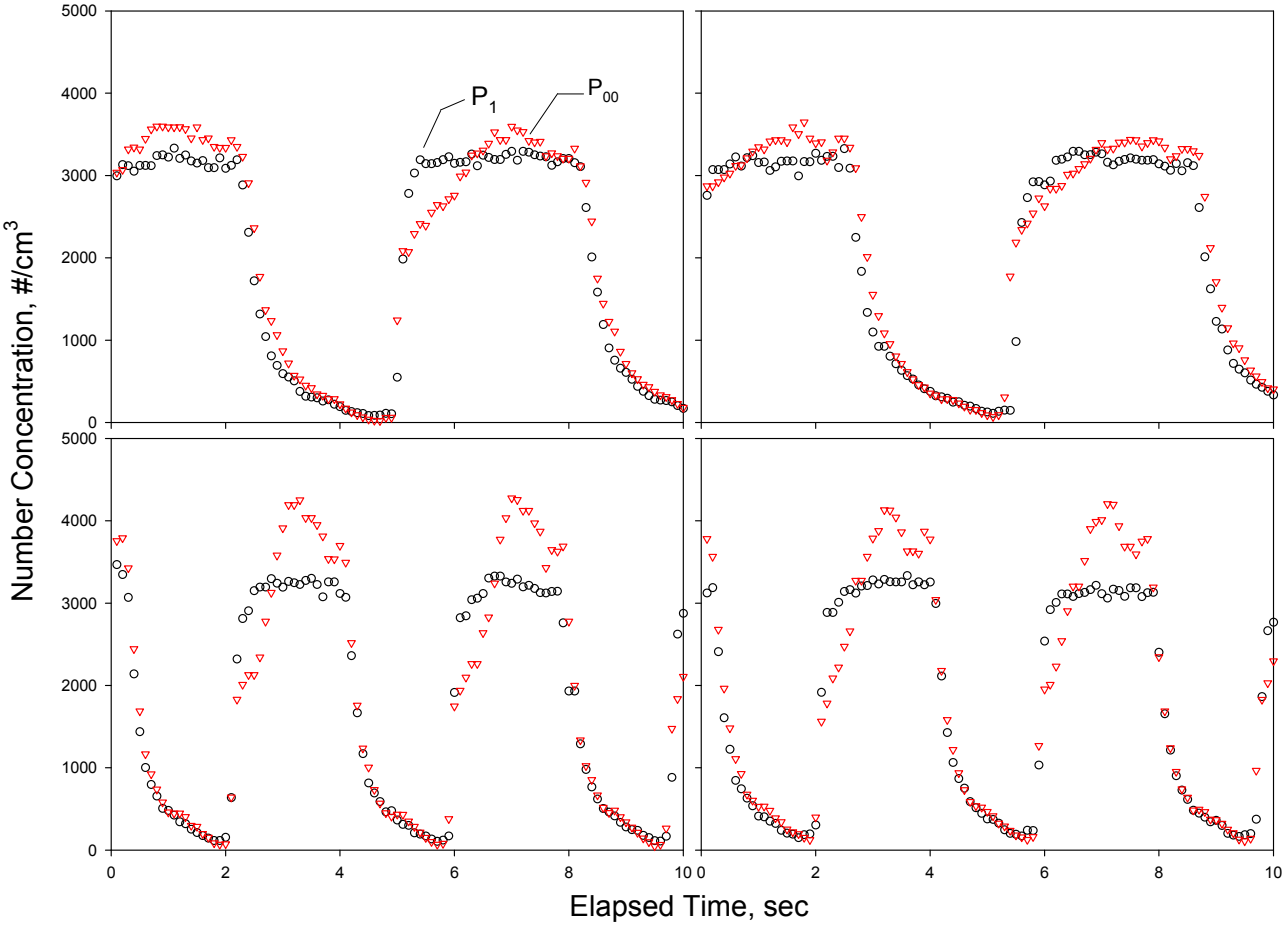

Fig. 7. Effect of breathing flow on the aerosol concentration measurement. The effect is particularly significant during inhalation, when small flow meter is used.

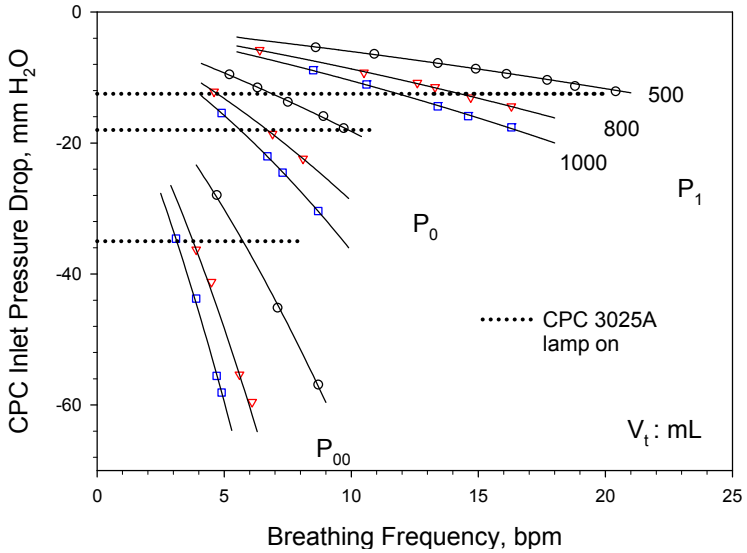

Fig. 8. Correlation of CPC inlet pressure drop and breathing frequency for three sampling probes at three tidal volumes.

gravitational settling becomes dominant. Therefore, the local deposition efficiency increases with volumetric lung regions. The limiting factor of this part of the experiment is that CPC does not size particles. If a high sampling rate aerosol spectrometer, such as 100 Hz of Welas 3000 (Palas Gmbh, Karlsruhe, Germany), can be employed, the regional deposition as a function of penetration volume can be resolved at an even higher resolution.

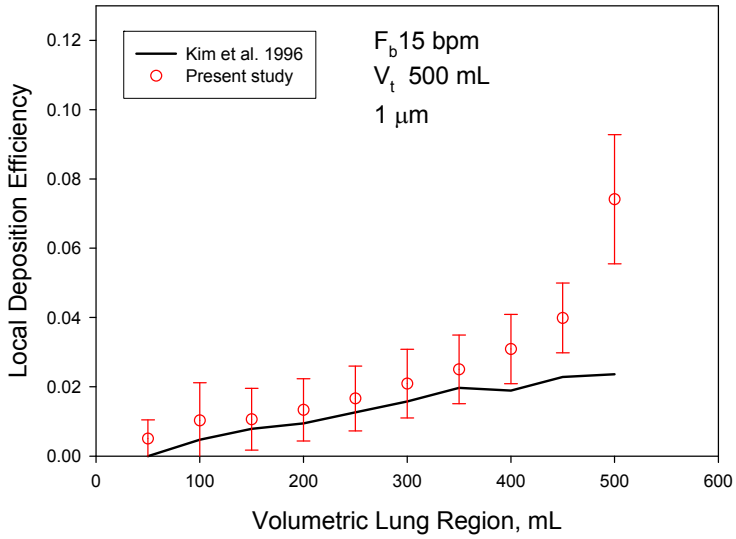

Fig. 9. Local deposition efficiency (for each 50 mL volumetric region) as a function of penetration volume.

Local deposition fraction was calculated as a function of penetration volume, as shown in Fig. 10. The trend of data collected in this work was similar to that of Kim's, but the deposition fraction was slightly higher. Since there was only one subject tested in the present study, the difference might not be of particular significance. The comparison of regional deposition data between the bolus technique (used by Kim) and the method adopted in this work will be published elsewhere.

CONCLUSIONS AND RECOMMENDATIONS

The experimental system for rapid measurement of regional lung deposition was successfully developed. This system functioned well at low particle concentration (1000–3000 #/cm^3). The condensation particle counters needed to operate under high flow mode to reduce the time lag to reach steady aerosol concentration. CPC 3025 has the fastest response time of all CPC models tested due to its small dead volume. The flow monitoring device showing the breathing pattern is critical to overall system performance. The pneumotachograph needs to generate a clear signal of breathing pattern for the subject to follow to obtain good quality lung deposition data. Among the flow meters tested in this work, the largest P_1 pneumotachograph is the only device suitable for normal breathing. Smaller pneumotachographs can only be used when the breathing flow (combination of breathing frequency and tidal volume) is lower than desirable.

The CPC flow rates fluctuated during the breathing cycle. A more powerful pump or external pump is needed for CPC to reduce this intrinsic error. We recommend aerosol size spectrometers with a sampling rate up to 100 Hz be investigated in the future. The high deposition efficiency in the deep lung is likely due to the 'dilution effect' of functional

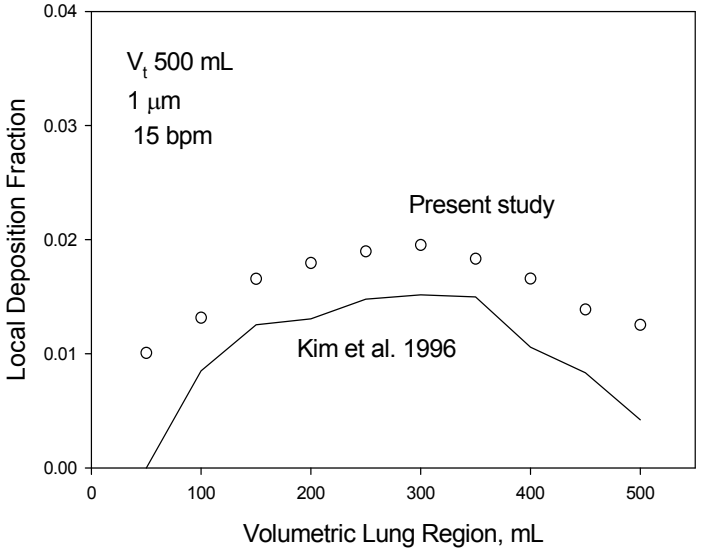

Fig. 10. Deposition fraction in local volumetric regions (for each 50-mL volumetric region) as a function of penetration volume.

residual capacity (FRC), where the aerosol concentration was expected to be low due to the long retention time in that region. This dilution effect needs to be validated, preferably with an advanced bolus system equipped with better breathing pattern control and aerosol counter.

ACKNOWLEDGEMENT

The authors would like to thank the National Science Council (Grant No. NSC 96-2221-E-002 -055 -MY3) and Institute of Occupational Safety and Health, Taiwan (Grant No. IOSH-100-H323), for the financial supports.

REFERENCES

Ali, M., Reddy, R.N. and Mazumder, M.K. (2008). Electrostatic Charge Effect on Respirable Aerosol Particle Deposition in a Cadaver Based Throat Cast Replica. *J. Electrostat.* 66: 401–406.

Anderson, P.J., Hardy, K.G., Gann, L.P., Cole, R. and Hiller, F.C. (1994). Detection of Small Airway Dysfunction in Asymptomatic Smokers Using Aerosol Bolus Behavior. *Am. J. Respir. Crit. Care Med.* 150: 995–1001.

Asgharian, B., Price, O.T. and Hofmann, W. (2006). Prediction of Particle Deposition in the Human Lung Using Realistic Models of Lung Ventilation. *J. Aerosol Sci.* 37: 1209–1221.

Blanchard, J.D. and Willeke, K. (1983). An Inhalation System for Characterizing Total Lung Deposition of Ultrafine Particles. *Am. Ind. Hyg. Assoc. J.* 44: 846–856.

Brand, P., Tuch, T., Manuwald, O., Bischof, W., Heinrich, J., Wichmann, H. E., Beinert, T. and Heyder, J. (1994). Detection of Early Lung Impairment with Aerosol Bolus Dispersion. *Eur. Respir. J.* 7: 1830–1838.

Brand, P., Rieger, C., Schulz, H., Beinert, T. and Heyder, J. (1997). Aerosol Bolus Dispersion in Healthy Subjects. *Eur. Respir. J.* 10: 460–467.

Brand, P., Haussinger, K., Meyer, T., Scheuch, G., Schulz, H., Selzer, T. and Heyder, J. (1999). Intrapulmonary Distribution of Deposited Particles. *J. Aerosol Med.* 12: 275–284.

Brand, P., Friemel, I., Meyer, T., Schulz, H., Heyder, J. and Haubetainger, K. (2000). Total Deposition of Therapeutic Particles during Spontaneous and Controlled Inhalations. *J. Pharm. Sci.* 89: 724–731.

Chan, T.L. and Lippmann, M. (1980). Experimental Measurements and Empirical Modelling of the Regional Deposition of Inhaled Particles in Humans. *Am. Ind. Hyg. Assoc. J.* 41: 399–409.

Cheng, Y.S., Yeh, H.C., Guilmette, R.A., Simpson, S.Q., Cheng, K.H. and Swift, D.L. (1996). Nasal Deposition of Ultrafine Particles in Human Volunteers and Its Relationship to Airway Geometry. *Aerosol Sci. Technol.* 25: 274–291.

Grgic, B., Martin, A.R. and Finlay, W.H. (2006). The Effect of Unsteady Flow Rate Increase on in Vitro Mouth-Throat Deposition of Inhaled Boluses. *J. Aerosol Sci.* 37: 1222–1233.

Hashish, A.H., Fleming, J.S., Conway, J., Halson, P., Moore, E., Williams, T.J., Bailey, A.G., Nassim, M. and Holgate, S.T. (1998). Lung Deposition of Particles by Airway Generation in Healthy Subjects: Three-Dimensional Radionuclide Imaging and Numerical Model Prediction. *J. Aerosol Sci.* 29: 205–215.

Heyder, J., Gebhart, J., Heigwer, G., Roth, C. and Stahlhofen, W. (1973). Experimental Studies of the Total Deposition of Aerosol Particles in the Human Respiratory Tract. *J. Aerosol Sci.* 4: 191–208.

Heyder, J., Armbruster, L., Gebhart, J., Grein, E. and Stahlhofen, W. (1975). Total Deposition of Aerosol Particles in the Human Respiratory Tract for Nose and Mouth Breathing. *J. Aerosol Sci.* 6: 311–328.

Heyder, J., Gebhart, J., Rudolf, G. and Stahlhofen, W. (1980). Physical Factors Determining Particle Deposition in the Human Respiratory Tract. *J. Aerosol Sci.* 11: 505–515.

Heyder, J., Blanchard, J.D., Feldman, H.A. and Brain, J.D. (1988). Convective Mixing in Human Respiratory Tract: Estimates with Aerosol Boli. *J. Appl. Physiol.* 64: 1273–1278.

Hofmann, W., Bergmann, R. and Koblinger, L. (1999). Characterization of Local Particle Deposition Patterns in Human and Rat Lungs by Different Morphometric Parameters. *J. Aerosol Sci.* 30: 651–667.

ICPR (1994). *Human Respiratory Tract Model for Radiological Protection*, Pergamon, Oxford.

Jaques, P.A. and Kim, C.S. (2000). Measurement of Total Lung Deposition of Inhaled Ultrafine Particles in Healthy Men and Women. *Inhal. Toxicol.* 12: 715–731.

Kim, C. and Jaques, P. (2004). Analysis of Total Respiratory Deposition of Inhaled Ultrafine Particles in Adult Subjects at Various Breathing Patterns. *Aerosol Sci. Technol.* 38: 525–540.

Kim, C.S., Hu, S.C., DeWitt, P. and Gerrity, T.R. (1996). Assessment of Regional Deposition of Inhaled Particles in Human Lungs by Serial Bolus Delivery Method. *J. Appl. Physiol.* 81: 2203–2213.

Kim, C.S. and Jaques, P.A. (2005). Total Lung Deposition of Ultrafine Particles in Elderly Subjects during Controlled Breathing. *Inhal. Toxicol.* 17: 387–399.

Kim, C.S. and Hu, S.C. (2006). Total Respiratory Tract Deposition of Fine Micrometer-Sized Particles in Healthy Adults: Empirical Equations for Sex and Breathing Pattern. *J. Appl. Physiol.* 101: 401–412.

Lippmann, M. and Albert, R.E. (1969). The Effect of Particle Size on the Regional Deposition of Inhaled Aerosols in the Human Respiratory Tract. *Am. Ind. Hyg. Assoc. J.* 30: 257–275.

Löndahl, J., Pagels, J., Swietlicki, E., Zhou, J., Ketzel, M., Massling, A. and Bohgard, M. (2006). A Set-up for Field Studies of Respiratory Tract Deposition of Fine and Ultrafine Particles in Humans. *J. Aerosol Sci.* 37: 1152–1163.

Luo, H.Y. and Liu, Y. (2009). Particle Deposition in a Ct-Scanned Human Lung Airway. *J. Biomech.* 42: 1869–1876.

McCawley, M. and Lippmann, M. (1988). Development of an Aerosol Dispersion Test to Detect Early Changes in

Lung Function. *Am. Ind. Hyg. Assoc. J.* 49: 357–366.

Möller, W., Felten, K., Seitz, J.G., Sommerer, K., Takenaka, S., Wiebert, P., Philipson, K., Svartengren, M. and Kreyling, W.G. (2006). A Generator for the Production of Radiolabelled Ultrafine Carbonaceous Particles for Deposition and Clearance Studies in the Respiratory Tract. *J. Aerosol Sci.* 37: 631–644.

Montoya, L., Lawrence, J., Murthy, G.K., Sarnat, J., Godleski, J. and Koutrakis, P. (2004). Continuous Measurements of Ambient Particle Deposition in Human Subjects. *Aerosol Sci. Technol.* 38: 980–990.

Park, S.S. and Wexler, A.S. (2007). Particle Deposition in the Pulmonary Region of the Human Lung: A Semi-Empirical Model of Single Breath Transport and Deposition. *J. Aerosol Sci.* 38: 228–245.

Park, S.S. and Wexler, A.S. (2008). Size-Dependent Deposition of Particles in the Human Lung at Steady-State Breathing. *J. Aerosol Sci.* 39: 266–276.

Rosenthal, F.S., Blanchard, J.D. and Anderson, P.J. (1992). Aerosol Bolus Dispersion and Convective Mixing in Human and Dog Lungs and Physical Models. *J. Appl. Physiol.* 73: 862–873.

Stahlhofen, W., Gebhart, J. and Heyder, J. (1980). Experimental Determination of the Regional Deposition of Aerosol Particles in the Human Respiratory Tract. *Am. Ind. Hyg. Assoc. J.* 41: 385–398.

Su, W.C. and Cheng, Y.S. (2006). Deposition of Fiber in a Human Airway Replica. *J. Aerosol Sci.* 37: 1429–1441.

Tu, K.W. and Knutson, E.O. (1984). Total Deposition of Ultrafine Hydrophobic and Hygroscopic Aerosols in the Human Respiratory System. *Aerosol Sci. Technol.* 3: 453–465.

Westenberger, S., Gebhart, J., Jaser, S., Knoch, M. and Köstler, R. (1992). A Novel Device for the Generation and Recording of Aerosol Micro-Pulses in Lung Diagnostic. *J. Aerosol Sci.* 23: 449–452.

Yu, C.P. and Diu, C.K. (1983). Total and Regional Deposition of Inhaled Aerosols in Humans *J. Aerosol Sci.* 14: 599–609.

Zhou, Y., Sun, J. and Cheng, Y.S. (2011). Comparison of Deposition in the USP and Physical Mouth-Throat Models with Solid and Liquid Particles. *J. Aerosol Med. Pulm. Drug Deliv.* 24: 277–284.

Received for review, July 12, 2012
Accepted, November 21, 2012